STUDY ON OPTIMIZED HULL FORM OF BASIC SHIPS USING OPTIMIZATION ALGORITHM

Hee-Jong Choi
Department of Naval Architecture and Ocean Engineering, Chonnam National University, Yeosu, South Korea.,
choihj@jnu.ac.kr

Dong-Woo Park
Department of Naval Architecture and Ocean Engineering, Tongmyong University, Busan, South Korea.

Myung-Soo Choi
Department of Maritime Police Science, Chonnam National University, Yeosu, South Korea.

Follow this and additional works at: https://jmstt.ntou.edu.tw/journal

Part of the Engineering Commons

STUDY ON OPTIMIZED HULL FORM OF BASIC SHIPS USING OPTIMIZATION ALGORITHM

Hee-Jong Choi[1], Dong-Woo Park[2], and Myung-Soo Choi[3]

ABSTRACT

In order to achieve minimum resistance for a ship hull, we used an optimization algorithm and computational fluid dynamics to develop a hull-form design. An ITTC 1957 model-ship correlation line formula was used to estimate the frictional resistance coefficient, and the wave-making resistance coefficient was evaluated by the Rankine source panel method with nonlinear free-surface boundary conditions. The geometry of the hull surface was represented and modified by a B-spline surface-modeling technique during the optimization process. Wigley and series 60 (C_B = 0.60) hulls were selected to obtain an optimized hull that produces minimum resistance. Experimental tests were carried out for the modified series 60 (C_B = 0.60) hull.

I. INTRODUCTION

Since the development of the landmark thin-ship theory of Michell (1898), considerable efforts have been devoted toward the development of computational fluid dynamics (CFD) techniques in order to predict ship resistance. The robust and practical CFD technique has been used as a replacement for the towing-tank test since CFD has advantages in terms of cost reduction and the quantity of detailed flow field information. Among CFD techniques, the potential-flow panel method based on Rankine sources with nonlinear free-surface boundary conditions is preferable in ship yards because of its simplicity and reduced computational cost despite its neglect of

viscosity (Abt et al., 2003; Lowe et al., 2003).

The resistance of a ship is determined by hydrodynamic forces, which strongly depend on the shape of the ship. Optimizing the hull form from the hydrodynamic point of view is a complicated problem, not only because of the many constraints imposed by practical demands but also because of the influence of surrounding conditions. Minimum operating fuel costs would be achieved by designing the hull for the best average performance over a range of conditions. This, however, is rarely feasible because of the current difficulties in quantifying the effect of all parameters involved and because of severe time constraints that are the rule in practical ship design.

Although some studies on hull-form optimization have provided some encouraging results, there are still a number of significant difficulties: selection of an appropriate objective function, choice of optimization scheme, geometric representation of hull surface and choice of a practical, robust CFD tool to evaluate the objective function, and the large computational cost to estimate the objective function through repeated computations during the entire optimization process.

Many interesting papers on hull-form optimization in terms of resistance have been published in recent years. Peri et al. (2001) presented several new optimized bulb shapes for a tanker with the aid of a potential flow solver and three different optimization algorithms. Markov et al. (2001) performed hull-form optimization for the series 60 (C_B = 0.60) hull and the Hamburg Test Case (HTC) container carrier using a potential flow solver (the higher-order Rankine source panel method) to evaluate the wave-making resistance, an unconstrained Davidson-Fletcher-Powell (DFP) formula as an optimization method, and a B-spline patch to approximate the hull surface during the optimization process. Zhang (2009; 2012) performed hull-form optimization using the Rankine source method to achieve the wave-making resistance as the objective function focusing on the optimization of the bow-body shape.

In the present study, hull-form optimization algorithm is proposed from the viewpoint of resistance reduction. To achieve the resistance of the ship, the wave-making resistance was computed using the potential-based panel method in which nonlinear-free surface boundary conditions and the trim and sinkage of a ship were fully taken into account, and

the friction resistance was estimated using the ITTC 1957 model-ship correlation line formula. During the optimization process, the geometry of the hull surface and the free surface was represented and modified by the B-spline surface model.

Numerical computations were performed to investigate the validity of the proposed algorithm. Wigley and series 60 ($C_B = 0.60$) hulls were used as reference hulls to derive the optimized hull form, and the optimized hull achieved as a result of the optimization process was manufactured and tested in a towing tank.

II. OPTIMIZATION ALGORITHM

1. General Optimization Problem

The general optimization problem can be expressed in the following form:

Minimize :

$$f(x) \tag{1}$$

Subjected to:

$$g_j(x) = 0, \quad j = 1, \cdots, m_e \tag{2}$$

$$g_j(x) \le 0, \quad j = m_e + 1, \cdots, m \tag{3}$$

$$x_l \le x \le x_u \tag{4}$$

where f is an objective function, g is a constraint function, x is the vector of the design variables, x_l and x_u are the lower and upper limits of x, m is the number of constraint functions, and m_e is the number of equality constraint functions.

2. Non-Linear Programming Algorithm

In the present study, Eqs. (1)-(3) are solved by a sequential quadratic programming algorithm, in which the equations are approximated in quadratic form:

Minimize :

$$\frac{1}{2} d^T B d + \nabla f(x)^T d \tag{5}$$

Subjected to:

$$\nabla g_j(x)^T d + g_j(x) = 0, \quad j = 1, \cdots, m_e \tag{6}$$

$$\nabla g_j(x)^T d + g_j(x) \ge 0, \quad j = m_e + 1, \cdots, m \tag{7}$$

where d is the search direction vector, and B approximates the Hessian matrix of the Lagrangian. During the optimization process, the optimum d is determined, and x is updated ac-

cording to $x^{n+1} = x^n + d$ in each iteration step (Vanderplaats, 1990).

III. EVALUATION OF OBJECTIVE FUNCTION

1. Potential-Based Panel Method

Define a Cartesian coordinate system that is fixed on a ship and translates with a constant speed, U. The x-axis points downstream and the z-axis points upwards. In this frame of reference, the ship is stationary experiencing an incoming uniform stream along the positive x-direction.

Flow is assumed to be incompressible, inviscid and irrotational, and governed by a velocity potential, ϕ subject to the Laplace equation in the fluid domain.

$$\nabla^2 \phi = 0 \tag{8}$$

Over the wetted part of the hull surface, the velocity potential must satisfy the hull boundary condition of zero flow normal to the hull surface.

$$\phi_n = 0 \tag{9}$$

n : Unit normal vector.

The radiation condition must be satisfied, as follows:

$$\nabla \phi \to (U, 0, 0) \text{ as } x^2 + y^2 + z^2 \to \infty \tag{10}$$

On the free surface, the kinematic and dynamic conditions must be satisfied according to the following equations

$$\phi_x \eta_x + \phi_x \eta_x - \phi_z = 0 \text{ on } z = \eta \tag{11}$$

$$\eta = \frac{1}{2g} \left(U^2 - \nabla \phi \bullet \nabla \phi \right) \tag{12}$$

η: Wave height
g: Gravitational acceleration

Because Eqs. (11)-(12) are fully non-linear, the iteration procedure should be adopted to solve the free-surface problem by employing the Rankine source panel method (Raven, 1992).

Having obtained the velocity potential and hence the flow velocity, the pressure coefficient, C_p at each panel can be determined using the Bernoulli equation

$$C_p = 1 - \frac{\nabla \phi \bullet \nabla \phi}{U^2} - 2\frac{z}{Fn^2} \tag{13}$$

$$Fn = \frac{U}{\sqrt{gL}} : \text{Froude number}$$

L: Length of the ship

The wave-making resistance coefficient, C_W is then given by the pressure integral over the wetted hull surface:

$$C_W = -\frac{\int_S C_p \, n_x \, ds}{S} \tag{14}$$

S: Wetted surface of the hull

The frictional resistance coefficient, C_F is given by the ITTC 1957 model-ship correlation line formula.

$$C_F = \frac{0.075}{(\log_{10} Rn - 2)^2} \tag{15}$$

$Rn = \dfrac{U\,L}{\nu}$: Reynolds number

ν: Kinematic viscosity

Finally the total resistance coefficient, C_T is obtained, as follows:

$$C_T = C_W + (1 + k)C_F \tag{16}$$

$(1 + k)$: Form factor

In Eq. (16), $(1 + k)$ is calculated using the empirical formula (Holtrop, 1984).

2. Panel-Cutting Method

In this method, hull panels are generated using only the initially selected hull panels, under the assumption that these initial hull panels are of the highest quality. We attempt to minimize the modification of the initial panels and make the best possible use of them (Choi et al., 2011).

To generate a hull panel, the positional relationship between a free surface and the four vertices of the panel should firstly be checked. If the panel is below the free surface, it is included in the numerical computation, whereas if it is above the free surface, it is not included. In a special case, the free surface intersects the panel, and the panel is then regenerated, albeit only the part that was submerged below the free surface.

In Fig. 1, the panels illustrated with a solid line are newly generated and included in the numerical computation, whereas those illustrated with a dotted line are not included. The numbers in Gothic type outside the panels are input sequences for the initially selected panels, and those in Italic type inside the panels are input sequences for the newly generated panels.

Fig. 1(a) shows a panel and free surface, where all four vertices of the panel are below the free surface, and the panel is included in the numerical computation. On the other hand, in Fig. 1(b), the panel is not included, because it is above the free surface.

In the hull-panel-generation process using the panel-cutting method, an intersection between the panel and the free surface
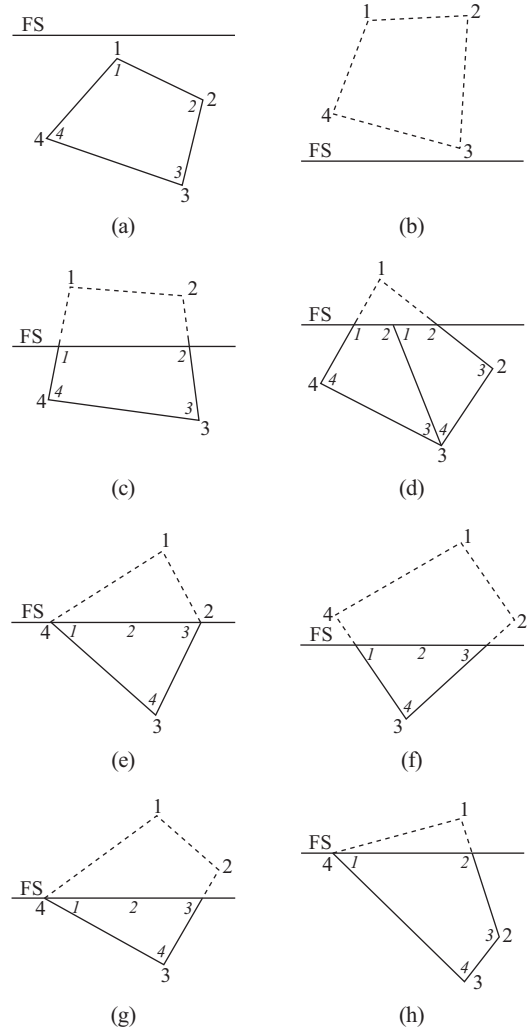

Fig. 1. Panel-cutting cases.

can occur. There are six possible intersection cases, as shown in Figs. 1(c)-(h). In Fig. 1(c), the panel is divided into two quadrilateral panels, of which, as previously mentioned, only the panel below the free surface is included in the numerical computation. In Fig. 1(d), a triangular panel is generated below the free surface. In Figs. 1(e) and (f), the 4th vertex is on the free surface, and a quadrilateral panel and triangular panel are generated, respectively. In Fig. 1(g), the 2nd and 4th vertices are on the free surface, and a triangular panel is generated. In Fig. 1(h), the panel is divided into a pentagonal panel and a triangular panel by the free surface, and the pentagonal panel is divided into two quadrilateral panels.

The newly generated panel could be too small for us to perform the numerical computation, owing to the performance of the computer: a fatal numerical error might occur. To avoid numerical difficulties, the panel less than 1/10 times the minimum panel is eliminated in the present study, and the minimum size of the panel should be determined according to the initially selected hull panels.

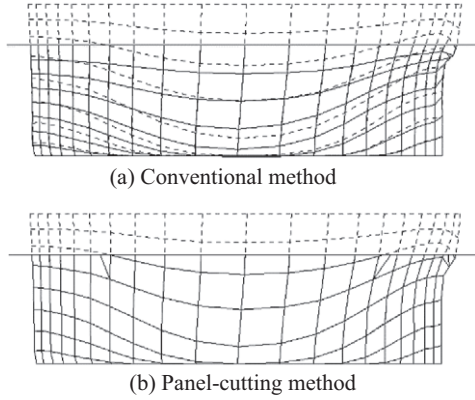Fig. 2(a) shows the initially selected hull panels of the

(a) Conventional method

(b) Panel-cutting method

Fig. 2. Comparison of panels generated using conventional method and panel-cutting method.

series 60 ($C_B = 0.60$) hull. Fig. 2(b) shows the newly generated hull panels according the undisturbed free surface and the wavy free surface.

IV. MODIFICATION OF HULL GEOMETRY

1. B-Spline Surface Modeling

An efficient algorithm for geometry modification is essential for the implementation of an optimization procedure. The modified geometry should meet the original design requirements without discontinuities in the surface and should generally be as smooth as possible.

For ship-hull optimization, it is necessary to use factors related to the hull-geometry generation as design variables. In this case, an increase in the number of design variables causes an increase in the computation time. If the number of design variables is too small, it may be difficult to obtain a realistic hull shape.

The following requirements were determined using a B-spline patch:

$$Q(u,v) = \sum_{i=1}^{n_i+1} \sum_{j=1}^{n_j+1} B_{i,j} \, N_{i,k}(u) M_{j,l}(v) \; , \qquad (15)$$

where $B_{i,j}$ represents the control vertices of a defining polygon net, and $N_{i,k}(u)$ and $M_{j,l}(v)$ are the B-spline basis function in the bi-parametric u- and v-directions, respectively. The basis functions is defined as follows:

$$N_{i,1}(u) = \begin{cases} 1 & if \;\; x_i \le u < x_{i+1} \\ 0 & otherwise \end{cases} \qquad (16)$$

$$N_{i,k}(u) = \frac{(u-x_i)N_{i,k-1}(u)}{x_{i+k-1}-x_i} + \frac{(x_{i+k}-u)N_{i+1,k-1}(u)}{x_{i+k}-x_{i+1}} \qquad (17)$$

and

$$M_{j,1}(v) = \begin{cases} 1 & if \;\; y_j \le v < y_{j+1} \\ 0 & otherwise \end{cases} \qquad (18)$$

$$M_{j,l}(v) = \frac{(v-y_j)M_{j,l-1}(v)}{y_{j+l-1}-y_j} + \frac{(y_{j+l}-v)M_{j+1,l-1}(v)}{y_{j+l}-y_{j+1}}, \qquad (19)$$

where x_i and y_j are elements of knot vectors.

2. B-Spline Surface Fitting

When the surface is described by external data, it is convenient to obtain an initial non-flat B-spline surface approximating the hull for subsequent real-time interactive modification. This requires determining the defining polygon net from an existing network of three-dimensional surface data points.

For each known surface data point, Eq. (20) provides a linear equation in terms of the unknown $B_{i,j}$ values. This can be expressed in matrix notation as

$$[D] = [C][B], \qquad (20)$$

where $C_{i,j} = N_{i,k} \, M_{j,l}$. For an arbitrary $r \times s$ topologically rectangular surface data point, $[D]$ is an $(r \times s) \times 3$ matrix comprising the three-dimensional coordinates of the surface data point, $[C]$ is an $(r \times s) \times (n \times m)$ matrix comprising the products of the B-spline basis functions, and $[B]$ is an $(n \times m) \times 3$ matrix comprising the three-dimensional coordinates of the required polygon net points.

Because for any arbitrary $r \times s$ topologically rectangular surface data point, $[C]$ is not normally square, only a rough solution can be obtained. In particular,

$$[B] = \left[[C]^T[C]\right]^{-1}[C]^T[D] \qquad (21)$$

The u and v parametric values for each surface data point are obtained using a chord length approximation (Huang et al., 1998; Rogers et al., 1990).

V. APPLICATION

The methods described above were applied to an optimization problem in which numerical computation had been performed using Wigley and series 60 ($C_B = 0.60$) hulls as the original hulls.

Wigley Hull

Since a potential flow solver was used to calculate the wave-making resistance as an objective function, the panels that define the shape of the ship surface should be generated at each iteration step during the whole optimization process. To make the optimization algorithm more stable for the numerical computation, the representation of the ship needed to be sufficiently flexible and robust to permit any type of hull-form
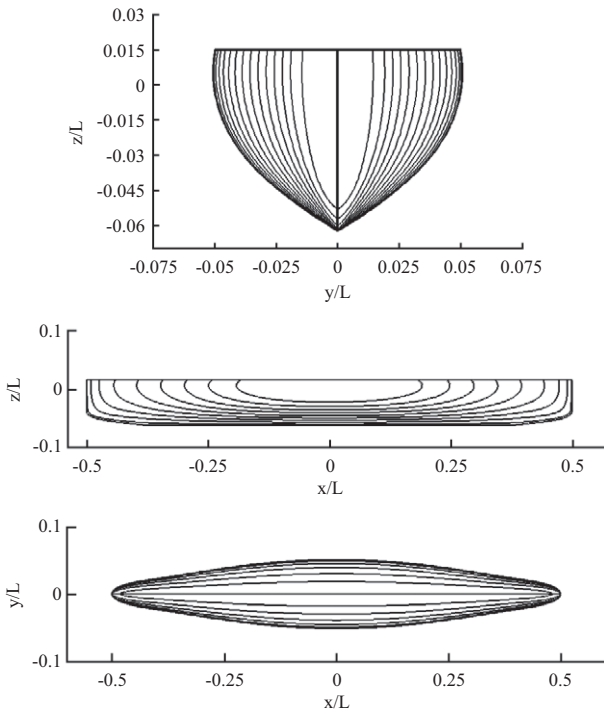
Fig. 3. Lines for the modified Wigley hull taken as original hull.

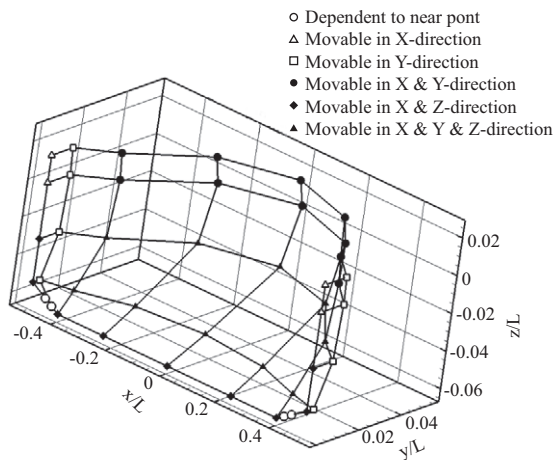
Fig. 5. Lines for the optimized Wigley hull.

Fig. 4. Design variables.

modification while simultaneously using only a moderate number of unknowns. That is an important factor in hull-form optimization because of the severe time constraints that are the rule in practical ship design.

Fig. 3 shows the body plan, the half-breadth plan, and the sheer plan of the modified Wigley hull, which was modified by the B-spline surface patch to maintain the continuity of the curvature across the center plane from the original Wigley hull.

1. Design Variables

Fig. 4 shows the control vertices network that was used as the design variables. The design variables were repositioned
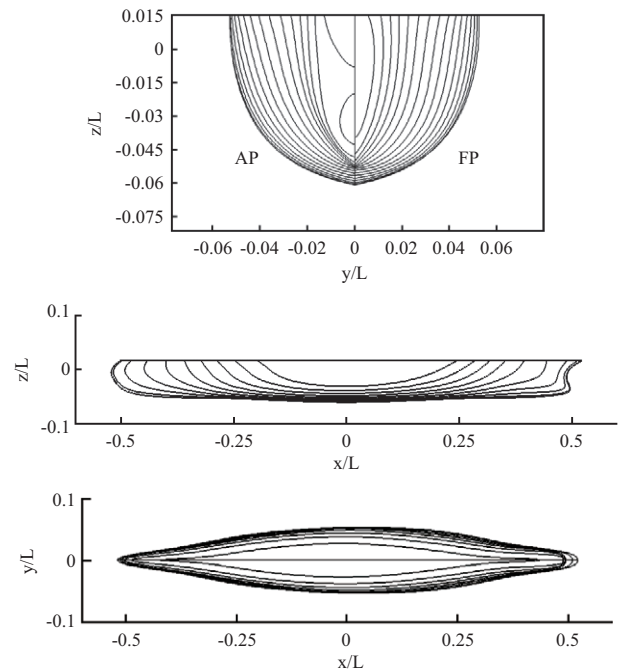
according to the optimization algorithm and used to generate the computation panel for numerical analysis. For the other zones, the control vertices were generated but not modified during the optimization process.

To maintain a reasonable ship shape, the range of the movement of the control vertices was also confined, as shown in Eq. (24).

$$-0.700 < x/L < 0.700$$

$$0.000 < y/L < 0.080$$

$$-0.080 < z/L < -0.010 \tag{24}$$

2. Computational Results

The numerical analysis was performed at the design speed of $Fn = 0.316$. The number of panels used in the numerical analysis was 3,690, which were distributed on the free surface (18×180) and on the hull (15×30).

Fig. 5 shows the body plan, the buttock line, and the waterline of the optimized hull. In the cases of the bow and stern, the lines can identify the evolution as the generation direction of the bulbous bow.

The wave profile of the optimized hull is compared with the wave profile of the original hull in Fig. 6, and the wave pattern of the optimized hull is compared with the wave pattern of the original hull in Fig. 7. The wave profile of the optimized hull shows the large reduction of the bow wave. The wave pattern of the optimized hull shows the large reduction of the wave over the entire range of the free-surface area as compared with the original hull. Especially, the wave

Table 1. Hydrostatic data and resistance for Wigley hull.

	Original	Optimized	Δ (%)
∇(displacement)	0.0028	0.0029	3.6
S_{WET}	0.1491	0.1401	-6.0
R_{WM}	0.1160	0.0231	-80.0
R_{TM}	0.4886	0.3734	-23.6
Sinkage (bow)	-0.0022	-0.0016	
Sinkage (stern)	-0.0022	-0.0025	
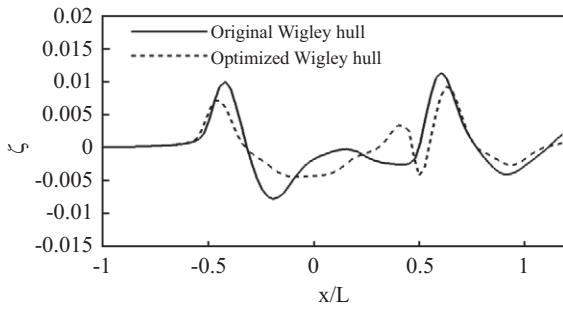
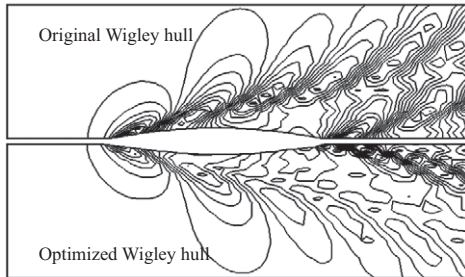Fig. 6. Wave profiles for the original hull and the optimized hull along the hull.

Fig. 7. The wave pattern for the original hull and the optimized hull.

that is generated on the bow shoulder of the hull shows noticeable reduction as compared with the original hull owing to the existence of the bulbous bow of the optimized hull.

Table 1 shows the volume displacement, the wetted surface area, the wave-making resistance, the total resistance, and the sinkage of the bow and the stern.

The series 60 ($C_B = 0.60$) hull

The method described above was applied to an optimization problem in which numerical computation had been performed using the series 60 ($C_B = 0.60$) hull as the original hull at the given design speed of $Fn = 0.316$ (Park et al., 2013).

3. Design Variables

As shown in Fig. 8, the ship surface was divided into two zones, and the ship optimization was only performed in the region 25% from the bow in which the flow was assumed to be the potential flow. Each zone was defined by the B-spline
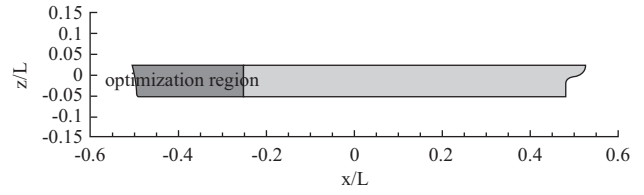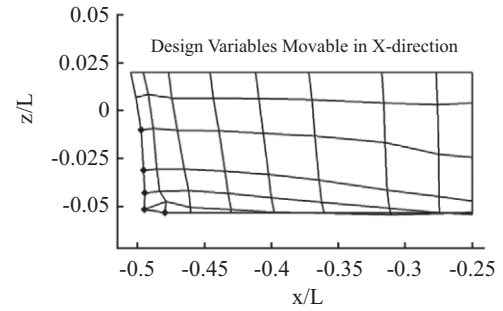

Fig. 8. Region to be optimized.

Fig. 9. Design variables varying in the x-direction.

surface patch. In the case of the optimization region, a surface patch with a 10×7 control net (7 control points for every 10 sections) was used to represent a hull form and the control vertices were used as design variables.

The design variables were repositioned according the optimization algorithm and used to generate the computation panel for numerical analysis. For the other zones, the control vertices were generated but not modified during the optimization process.

Fig. 9 shows the control vertices that were allowed to move in the x-direction. The control vertices at the first and second sections had the same x-coordinates at each row to enforce continuity of curvature across the center plane.

$$-0.550 \ < x/L \ < -0.475 \tag{25}$$

As the control vertices moved in the x-direction, the x-coordinates of the other control vertices between the second and last sections moved inversely proportional to the distance between the two points. To maintain a reasonable hull form shape, the range of the movement of the control vertices was confined as shown in Eq. (25).

Fig. 10 shows the design variables that were allowed to move in the y-direction. To maintain a reasonable ship shape, the range of the movement of the control vertices was also confined as shown in Eq. (26).

$$0.0000 < y/L < 0.0300 \tag{26}$$

4. Constraint Conditions

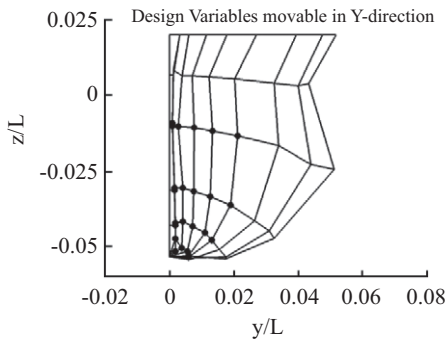The constraints of the volume displacement and the wetted surface area of the ship were pre-described depending on the

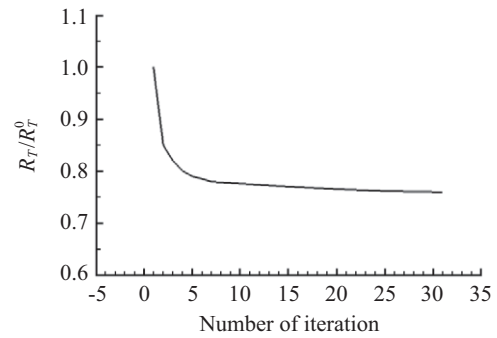**Fig. 10. Design variables varying in the y-direction.**

Fig. 11. Convergence history.

requirements of the ship designer since they are most important factors in ship design.

In the present study, the constraint for the volume displacement was set as follows, which might be a severe penalty from a resistance point of view:

$$\nabla \geq \nabla_{original\ hull} \qquad (27)$$

The constraint for the normal vector to the hull surface was applied to avoid the evolution of the hull in an undesirable direction.

$$n_x \leq 0, \ n_y \geq 0 \qquad (28)$$

n_x: x-component of unit vector normal to the hull surface
n_y: y-component of unit vector normal to the hull surface

The constraints given in Eq. (28) are important since all numerical computations during the optimization process were performed automatically so that the ship had a reasonable hull shape without external modification. During the optimization procedure, it was found that the numerical computations were more stable and the ship shape could be more smoothly modified in a smoother way by enforcing the constraints.

5. Computational Results

The numerical analysis was performed at a design speed of $Fn = 0.316$. The number of panels used in the numerical analysis was 5,040, which were distributed on the free surface (18×180) and on the hull (30×60).

Fig. 11 shows the variation of R_T / R_T^0 with respect to the number of iterations. Here, R_T^0 is the total resistance for the original hull form. As shown in Fig. 11, the total resistance was quickly reduced during the first five iterations, after five iterations the reduction rate slowly decreased and finally converged. The computation time depends on the number of design variables, in this case, the time used in each iteration was approximately 30 minutes.

The volume of the middle of the bow increased dramatically and the bow became bulb-shaped as compared with the
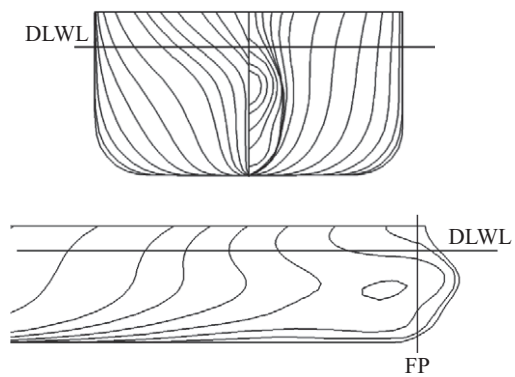

Fig. 12. The body plan and buttock line for the optimized hull.
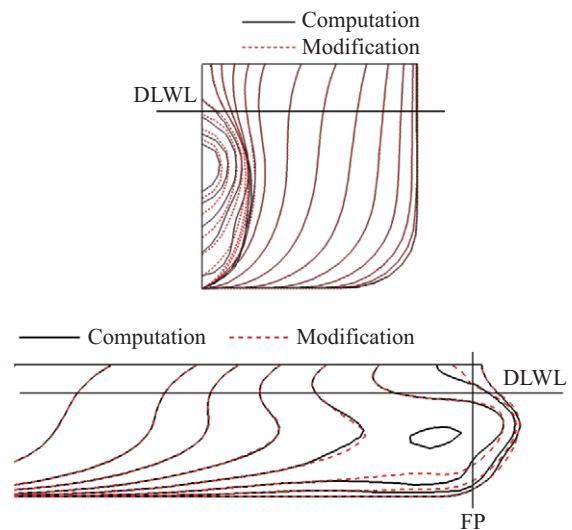

Fig. 13. The optimized hull and the modified optimized hull.

original hull, as shown in Fig. 12. Although some constraints were provided to prevent undesirable hull-form generation, it is still noticed that there are some unusual curves that seem impractical. The optimized hull was, therefore, slightly modified manually using a surface-fitting technique.

Fig. 13 shows a comparison between the optimized hull and the final version of the optimized hull with slight modification.
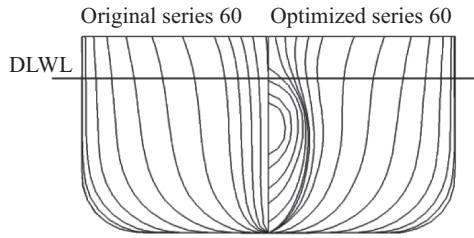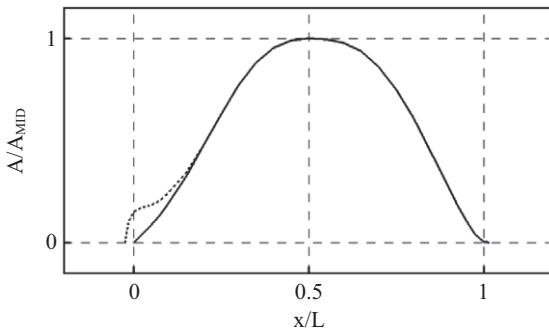
Fig. 14. Comparison of the body plans.

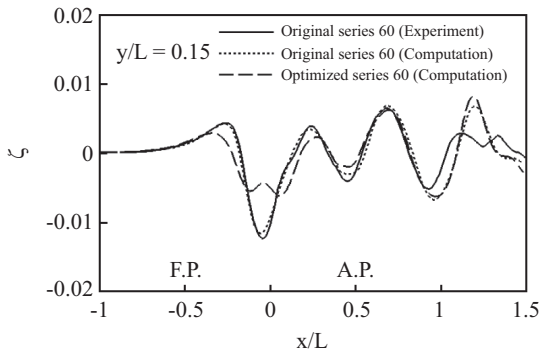**Fig. 15. Comparison of the sectional area curves.**

Fig. 16. Comparison of the wave profiles at y/*Lpp* = 0.08 (*Fn* = 0.316).

Fig. 17. Comparison of the wave contours (*Fn* = 0.316).

Fig. 18. Model of the optimized series 60 (*C_B* = 0.60) hull.
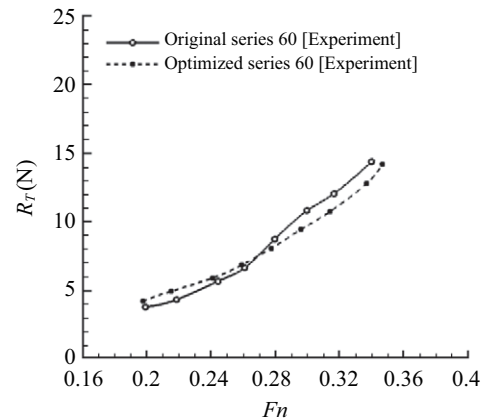
Fig. 19. Comparison of the total resistances (*R_T*).

Great care was taken to maintain the main features of the optimized hull.

The body plans of the original hull and the optimized hull are compared in Fig. 14 and the sectional area curves are compared in Fig. 15. The optimized hull has a large bulb as compared with the original hull.

In Fig. 16, the wave profiles in the longitudinal direction in the vicinity of the hull were compared and the measured wave profile of the original hull was also compared with the computed results. For the original hull, the computed results predicted slightly larger wave heights than the measured data near the stern. This is because the potential flow solver ignores the viscosity of the fluid. The wave height in the bow of the optimized hull was considerably reduced primarily because of the existence of the bulb. Over the entire free-surface area, the wave height was reduced, as shown in Fig. 17.
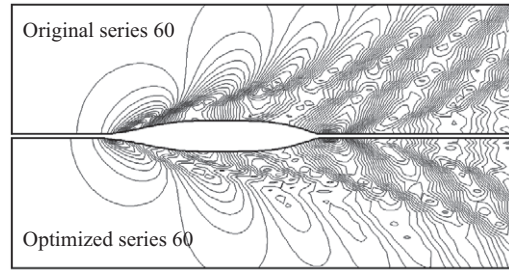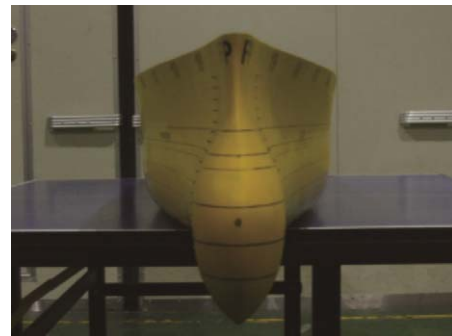
## 6. Experimental Validation

A model test was carried out for the original hull and the optimized hull. Fig. 18 shows the model of the optimized hull. The length of the model of the original series 60 (C_B = 0.60) hull is 3.5 *m*, and the breadth is 0.467 *m*, and the draft is 0.187 *m*.

As shown in Fig. 19 and in Table 2, the total resistance was reduced by 13.3% as compared with the original hull at the design speed, and the wetted area and total volume of the optimized hull were increased by 0.9% and 2%, respectively.

In Fig. 20, the residuary resistance of the optimized hull was reduced by approximately 40% while the computational result shows 26.5% reduction, where the residual resistance

Table 2. Comparison of the hydrostatic/dynamic data.

	Hull form		Original	Optimized	Δ (%)
	∇	(m^3)	0.115	0.117	2.0
	S_{WET}	(m^2)	1.539	1.553	0.9
Computation	C_W	(10^3)	1.860	1.360	-27.1
	R_W	(N)	0.156	0.115	-26.5
Experiment	C_R	(10^3)	2.040	1.220	-40.5
	R_{RM}	(N)	4.620	2.820	-39.1
	R_{TM}	(N)	12.48	10.83	-13.3
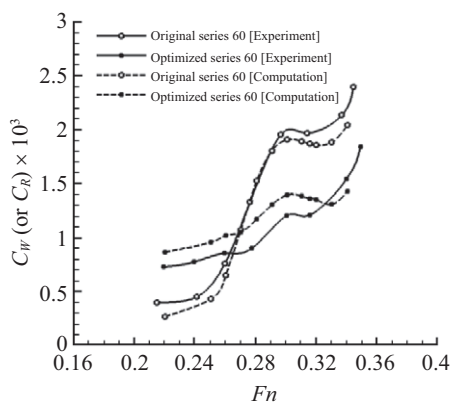
Fig. 20. Comparison of the residual/wave-making resistance coefficients (C_{RM}/C_W).

was calculated by subtracting the frictional resistance calculated using the ITTC 1957 model-ship correlation line from the total resistance.

VI. CONCLUSION

The hull optimization algorithm was applied to the Wigley and series 60 ($C_B = 0.60$) hulls as the original hulls and generated an optimized hull form in terms of the minimum resistance. Model tests were performed to validate the applied algorithm, and the computed results were compared with the experimental results.

The optimized hull form of the Wigley hull showed a total resistance gain of -23.6% as compared with the total resistance of the original hull form. The experimental results of the series 60 ($C_B = 0.60$) hull form showed that the optimized hull gave a 13% reduction in the total resistance and a 40% reduction in the residuary resistance. It should be noticed, however, that the reduction rate of the resistance mostly depends on choosing the original hull. The results indicate that the proposed optimized algorithm and the constraint conditions might be effectively applied to design a better hull form. It was shown that a change in the bow hull form of two ships, although it is a small fraction of the total hull geometry, might result in critical changes in wave pattern and subsequently in the total resistance performance of the two ships.

REFERENCES

Abt, C., S. Harries, J. Heimann and H. Winter (2003). From redesign to optimal hull line by means of parametric modeling. 2nd International on Computer Applications and Information Technology in the Marine Industries (COMPIT 2003), Hamburg, German, 444-458.

Choi, H. J., H. H. Chun, I. L. Park and J. Kim (2011). Panel cutting method: new approach to generate panels on a hull in Rankine source potential approximation. International Journal of Naval Architecture and Ocean Engineering 3(4), 225-232.

Holtrop, J. (1984). A statistical re-analysis of resistance and propulsion data. International Shipbuilding Progress 31(363), 272-276.

Huang, C. H., C. C. Chiang and S. K. Chou (1998). An inverse geometry design problem in optimizing hull surfaces. Journal of Ship Research 42(2), 79-85.

Lowe, T. W. and J. Steel (2003). Conceptual hull design using a genetic algorithm. Journal of Ship Research 47(3), 222-236.

Markov, N. E. and K. Suzuki (2001). Hull form optimization by shift and deformation of ship sections. Journal of Ship Research 45(3), 197-204.

Michell, J. H. (1898). The wave resistance of a ship. Philosophical Magazine Series 5, 45(272), 106-123.

Park, D. W. and H. J. Choi (2013). Hydrodynamic hull form design using an optimization technique. International Journal of Ocean System Engineering 3(1), 1-9.

Peri, D., M. Rosetti and E. F. Campana (2001). Design optimization of ship hulls via CFD techniques. Journal of Ship Research 45(2), 140-149.

Raven, H. C. (1992). A practical nonlinear method for calculating ship wave-making and wave resistance. Proceeding of 19th ONR Symposium on Naval Hydrodynamics, Seoul, Korea, 349-370.

Rogers, D. F. and J. A. Adams (1990). Mathematical Elements for Computer Graphics. McGraw-Hill, New York.

Vanderplaats, G. N. (1984). Numerical Optimization Techniques for Engineering Designs. McGrow-Hill, New York.

Zhang, B. J. (2009). The optimization of the hull form with the minimum wave making resistance based on Rankine source method. Journal of Hydrodynamics 21(2), 277-284.

Zhang, B. J. (2012). Research on optimization of hull lines for minimum resistance based on Rankine source method. Journal of Marine Science and Technology 20(1), 89-94.